

Compositional dependence of the electronic properties of amorphous Te-Tl^{†*}

M. A. Paesler[†]

Department of Physics, The University of Chicago, Chicago, Illinois 60637

(Received 14 January 1976)

The behavior associated with chemical ordering in thin amorphous films of $\text{Te}_m\text{Tl}_{1-x}$ deposited and measured on 77-K substrates has been studied by transport, optical, Auger, and other experiments. It was determined from the high-temperature conductivity and the transmission in the near infrared, that the principal bonding in Te_mTl_2 is independent of composition over the range studied ($1.8 < m < 3.8$). The dc conductivity at integral m has typical semiconducting values ($\sim 10^{-8} \Omega^{-1} \text{cm}^{-1}$ at 77 K) but at half-integral m the samples are as many as seven orders of magnitude more conductive. This strong compositional dependence is interpreted to be due to a peak in the density of electronic gap states near the Fermi level that occurs in films of half-integral m . These states may be annealed from oxygen-free films but are locked into samples containing a few atomic percent of oxygen.

I. INTRODUCTION

A few years ago Ferrier *et al.*¹ discovered drastic variations of the electrical conductivity and its activation energy as a function of composition in thin amorphous films of the binary system Te-Tl. The dc conductivity measured at 77 K suggested that the material changed nine times from metallic to semiconducting behavior, with the latter occurring at compositions Te_mTl_2 for $m=1, 2, \dots, 7$ as well as at Te_2Tl_3 and Te_5Tl_3 . The amorphous films were nearly metallic about halfway between each of these compositions. Although some chemical ordering occurs in many amorphous binary or pseudobinary systems with extrema in the compositional dependence of the physical properties, no other system is known which exhibits chemical ordering at so many compositions. And in no other system is nearly-metallic behavior seen at compositions halfway between those of compound formation. For these reasons we decided to reexamine these phenomena and to extend the investigation to include additional charge transport and optical experiments.

If one considers a material to be chemically ordered (or chemically bonded) when an aggregate exists with sufficient stability to make it convenient to consider it an independent molecular species, then amorphous Te-Tl certainly represents a chemically ordered system. At another extreme, As-Te is often cited as an amorphous system with very little chemical order. Using the bond energies determined by Pauling² one finds that the As-As, Te-Te, and As-Te bonds are all of similar strengths so one might expect that all bonds would occur with their compositional probability. Experimentally, this appears to be the case. As a function of composition x , measured optical³ and thermodynamic⁴ properties of $\text{As}_x\text{Te}_{1-x}$ show fea-

tureless monotonic behavior.

There are, of course, materials exhibiting physical properties with compositional dependences lying between these extremes. For example, in other arsenic chalcogenides⁵ distinct features in plots of the compositional dependence of physical properties occur at 40-at.% arsenic where a molecular species is known to exist in the corresponding crystalline material.

The unique Te-Tl binary system presents interesting questions fundamental to our understanding of both chemical ordering and the structure of the electronic density of states in amorphous semiconductors. In the following, we discuss the problem presented by the Te-Tl system and propose several experiments aimed at shedding light on this problem. We show how the outcome of these investigations led us to further experiments and then describe how their results both contribute to our understanding of conductive processes in amorphous semiconductors and pose new questions basic to our understanding of these materials.

II. THE PROBLEM

One might not *a priori* expect any of the physical properties of thin solid films of Te-Tl to exhibit strong compositional dependence since such effects are uncommon in high- Z materials. The *liquid* Te-Tl system, however, has been extensively studied and the effects of chemical ordering have long been established. For example, investigations by Cutler⁶ have determined that for a broad range of temperatures liquid $\text{Te}_x\text{Tl}_{1-x}$ alloys exhibit properties that can be attributed to chemical ordering. A maximum in resistivity at the composition $x=0.33$ demonstrates the stability of the structural unit TeTl_2 . For $x < 0.33$, it is generally accepted that one is dealing with a dilute metal alloy of

TeTl_2 molecules and Tl^{3+} ions, while for $x > 0.33$, Cutler⁷ argues that the behavior of the compositional dependence of the conductivity can be attributed to broken Te-Te bonds. In any case, the stability of TeTl_2 is manifest in the liquid system.

It is quite often the case in disordered systems that the effects of chemical ordering can be enhanced by annealing. A chemically ordered configuration may be thought of as being a metastable state that a system would relax into when annealed. During this process strong bonds are made at the expense of weak bonds thereby lowering the total energy of the system.

Armed with a knowledge of the behavior of the liquid Te-Tl system and the nature of chemical bonding in general, one might thus expect disordered films of $\text{Te}_x\text{Tl}_{1-x}$ to exhibit some chemical ordering effects. It might be further expected that any observed effects would be enhanced by annealing. In these two regards the results of Ferrier *et al.* (FPA) can be anticipated, however, the drastic variations in conductivity seen in Fig. 1 are not expected. In particular, the data of Fig. 1 present

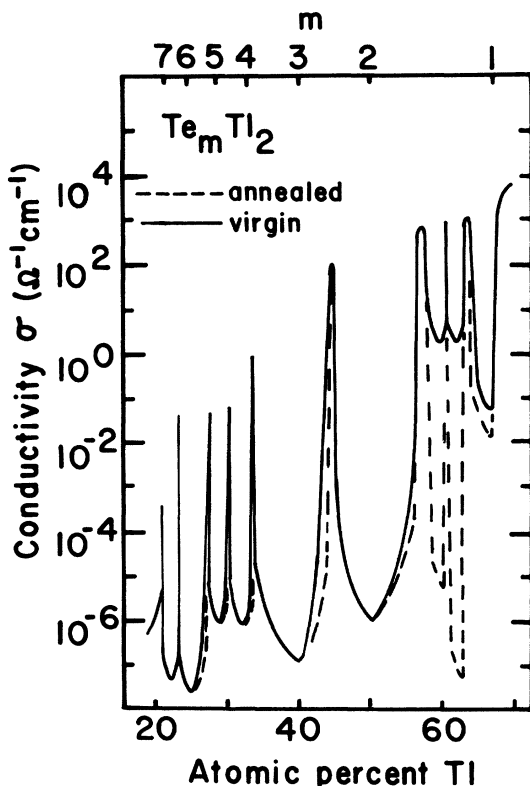


FIG. 1. Compositional dependence of the dc conductivity σ of virgin and annealed samples of Te_mTl_2 deposited on 77-K substrates as reported by Ferrier *et al.* (Ref. 5). Broad conductivity minima occur at compositions corresponding to integral values of m , while sharp maxima occur at half-integral m . These effects of chemical ordering are enhanced upon annealing.

us with a problem unique in the study of chemically ordered amorphous semiconductors.

If one concludes from the data of Fig. 1 that the Te-Tl system is comprised of mixtures of units Te_mTl_2 , then the strong variation of the conductivity as a function of composition seems to indicate that at composition m , only the structural unit Te_mTl_2 exists. If it were possible to have a mixture of $\dots, m-1, m, m+1, \dots$ units at composition m , then this mixture would be different from that at $(m + \frac{1}{2})$ only in a shift of the center of the distribution. The fact that integral and half-integral composition materials behave so differently suggests that at m only the unit Te_mTl_2 exists. At compositions corresponding to half-integral m , one would expect a mixture of units Te_mTl_2 and $\text{Te}_{m+1}\text{Tl}_2$. This is a pseudobinary mixture and we know of no other case in which a mixture of two saturated bond semiconductors becomes highly conductive. Bonds can be satisfied by forming a mixture of the end members of the pseudobinary, and if the bonds are satisfied, one expects an amorphous semiconductor with a conductivity not greatly unlike that of the two constituent structural units. FPA find that at integral composition m , the activation energies for conduction do not vary appreciably as a function of m . Thus the conduction mechanism appears to be of the same character for all integral m . Yet when viewed as constituents of a pseudobinary, two units of integral composition can result in a mixture seven orders of magnitude more conductive than either of the constituents.

We began our work on the Te-Tl system in an effort to shed some light on the answers to the questions posed by this system. In determining an experimental line of attack, we first formulated two models which could explain the data seen by FPA and then proposed experimental checks for each model.

The first of these models involves a charge transfer mechanism. We consider the structural units to be chains of different lengths m , $\text{Tl}-(\text{Te})_m-\text{Tl}$, and suppose that chemical ordering occurs because the chain energy is not linear in chain length. For longer chains the negative charge transferred from the Tl atoms can spread out over more electronegative Te atoms and the repulsion between the Tl atoms is less. At compositions $m=1, \dots, 7$ the bonds are saturated and the material is thus semiconducting. On the other hand, compositions deviating from whole m numbers require a mixture of chain lengths. Since the electronic charges transferred to the Te chain are held closer together in a shorter chain, we might imagine that the larger repulsive force between these charges might result in an ionization

energy less than that of a longer chain. Thus in a compound comprised of a mixture of chain lengths, we suppose that some charge transfer from shorter to longer chains is likely. With the addition of $(m+1)$ chains to (m) chains the Fermi level will move toward the valence band of the (m) chains. At small $(m+1)$ chain concentrations the transferred charge to these chains will be localized. By the same token, addition of a few (m) chains to a majority of $(m+1)$ chains will raise the Fermi level toward the conduction band of the $(m+1)$ chains. In the first case the $(m+1)$ chains act as acceptors in an (m) chain host, while in the latter case the (m) chains act as donors in an $(m+1)$ chain host. At the 50-50 mixture, one obtains a disordered charge transfer solid which is well conducting.

We have only sketched this model in its simplest form, leaving out correlation effects, Coulomb interactions between the polar Te-Tl bonds and other complicating factors. Nevertheless even for this simple model, experimental verification is possible. Since the thermopower S is a measure of the sign of the dominant charge carrier, a straightforward check of the validity of this model could be obtained by measuring the compositional dependence of S . If the movement of the Fermi level is as we have described it above, S should change appreciably as a function of composition. In fact since in most amorphous semiconductors one finds the Fermi level near mid-gap, we would not be surprised to find a change in sign of S near integral m compositions. Thus to check this model we proposed an experimental determination of the thermopower as a function of composition.

An alternative model supposes that $(m + \frac{1}{2})$ material might be very differently bonded than a mixture of (m) material and $(m+1)$ material. Different bonding would reflect itself in differences in the electronic density of states and thus could lead to the extreme changes in conductivity seen in Fig. 1. Such bonding changes would also manifest themselves in changes in the optical absorption edge E_g and the index of refraction. For example in thin evaporated films of amorphous As_2S_3 there is a shift of E_g towards lower energies upon annealing.⁸ This is interpreted as reflecting a change from a molecular solid containing As_2S_6 units to a polymerized cross-linked glass. Thus to check the validity of this explanation for the behavior shown in Fig. 1, we decided to measure the optical absorption constant and the index of refraction as a function of composition.

The experimental plan of attack aimed at addressing ourselves to the problems presented by this system thus involves determining the dc conductivity, thermopower, optical absorption constant

and index of refraction of thin amorphous films of Te_xTl_{1-x} as a function of composition. These experiments are complicated by the fact that the films must be deposited on liquid nitrogen cooled substrates and measured *in situ*.

If it proves to be the case that neither of the two proposed models provides us with an accurate picture of charge transport in amorphous Te_xTl_{1-x} films, the proposed experiments will reveal much about the electronic density of states of the system. Since this system is in many ways quite unusual, knowledge of its electronic density of states may provide useful clues about the nature of the density of states of amorphous semiconductors in general.

III. EXPERIMENTAL PROCEDURE

A. Transport measurements

By coevaporating Te and Tl from separate sources, it was possible with proper substrate placement to obtain in one evaporation a series of films of slightly different compositions. Since the conductivity maxima were expected to be quite sharp, this configuration was also chosen to increase our chances of obtaining data at the maxima. In such a configuration, Tl was evaporated from a tungsten boat while Te was evaporated from a cylindrical quartz cell with a small (~1 mm) opening at the top. This type of source⁹ makes it possible to keep the surface to volume ratio of the charge quite small thus reducing the possibility of evaporating a surface oxide of Te rather than pure Te. The cell was heated by passing a current through a tungsten coil wound around the quartz cylinder. Impurity levels in the charge material were ≤ 10 ppm. In a diffusion pumped system with a base pressure of better than 2×10^{-7} Torr, 1-2- μ m-thick films were deposited at a pressure of approximately 2×10^{-6} Torr and at an evaporation rate of approximately 40 Å/sec.

Deposition was monitored with two quartz oscillators—one for each source. Calibration samples were deposited on Dow Corning 7059 glass and dissolved upon completion of each experiment for compositional analysis with a Perkin Elmer model 603 atomic flame spectrometer. The expected composition of each sample was calculated from the frequency shifts of the oscillators. In Fig. 2 we show the calculated curve for the ratio of the frequency shifts $(\Delta f_{Te}/\Delta f_{Tl})$ versus composition. The calculated expected composition and the measured composition of the calibration sample were within 2 at.% of each other as can be seen for the three points shown.

For transport measurements, coplanar palladium electrodes¹⁰ were sputtered onto sapphire sub-

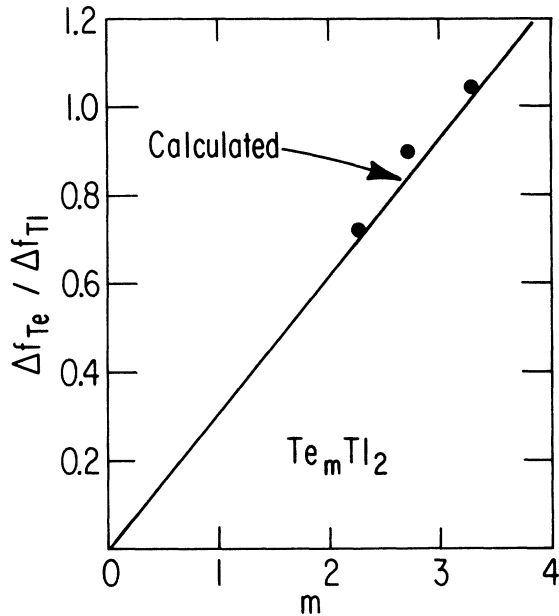


FIG. 2. Calculated and observed compositions of films of Te_mTl_2 vs the ratio of deposition monitor frequency shifts ($\Delta f_{\text{Te}}/\Delta f_{\text{Tl}}$). For a given ratio $\Delta f_{\text{Te}}/\Delta f_{\text{Tl}}$ we calculate the expected composition of our films and show this as the solid line. The points shown represent the measured compositions of three typical samples as determined by atomic flame absorption spectroscopy. The calculated and observed compositions always lie within two atomic percent of one another.

strates mounted to a Dewar which extended into the vacuum system. Construction was such as to allow control of the sample temperature and the thermal gradient across the sample from 77 to 300 K. The optical measurements were accomplished *in situ* by constructing a hinged Dewar extension for mounting sapphire substrates. The substrate could be held horizontally for deposition from below and then moved to a vertical orientation for the optical transmission measurements. Temperature control from 110 to 300 K was possible. Substrate temperature was measured with chromel-alumel thermocouples soldered to the sapphire.

The results of our measurements¹¹ of the conductivity as a function of composition for virgin samples of Te_mTl_2 deposited and measured at 77 K are shown in Fig. 3. For these samples, our data agree quite well with the published data of FPA. The broad minima at integral m and the sharp maxima at half-integral m are reproduced accurately.

We were quite surprised, however, to find that for annealed samples prepared as described above, the results of FPA cannot be reproduced. Upon annealing the effects attributed to chemical ordering no longer exist. That is, all samples are quite

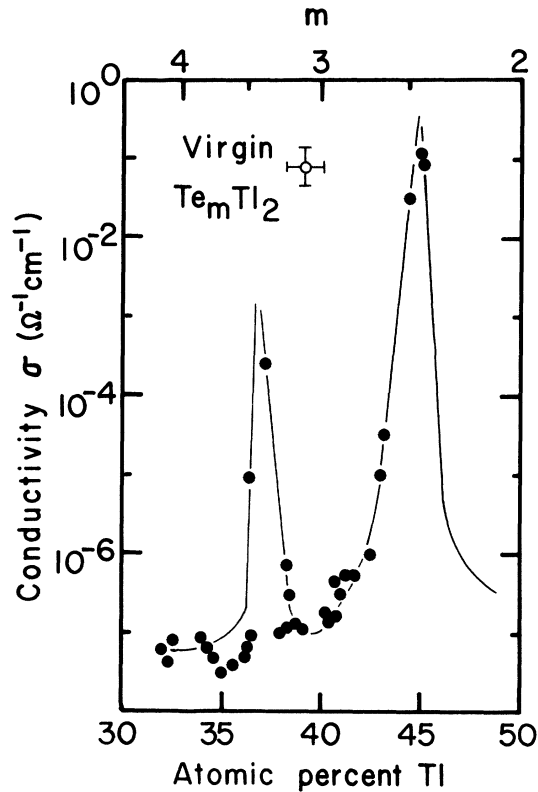


FIG. 3. Compositional dependence of the dc conductivity σ of virgin coevaporated samples of Te_mTl_2 deposited on 77-K substrates. For virgin samples, the features of Fig. 1 are reproduced. Typical error bars are shown on the open circle.

resistive and the maxima seen in Fig. 3 disappear.

This behavior is illustrated in Fig. 4 where we plot the conductivity σ of one of our more conductive samples versus inverse temperature $1/T$. After deposition at 77 K, σ at any given T becomes more and more resistive as subsequently higher annealing temperatures are reached until approximately 150 K where the annealing effects have saturated. Upon reaching this temperature, the sample no longer anneals and its $\sigma(T)$ curve can be retraced reproducibly as the temperature is cycled up and down until the sample crystallizes and becomes quite conductive at its crystallization temperature $T_c = 190$ K. Samples that are resistive when deposited exhibit conductivity curves very similar to that shown for the fully annealed sample of Fig. 3.

For the temperature range spanned by these experiments, it is convenient to describe the conduction with the expression

$$\sigma = C \exp(-\Delta E/kT), \quad (1)$$

where k is Boltzmann's constant and ΔE is the activation energy for conduction. The prefactor C

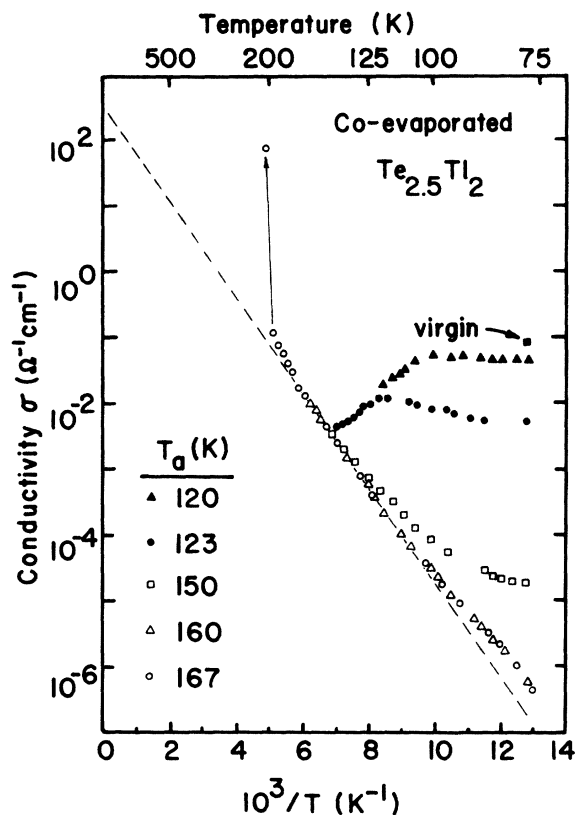


FIG. 4. Temperature dependence of the dc conductivity of coevaporated films of $\text{Te}_{2.5}\text{Tl}_2$. As higher annealing temperatures are reached for each successive heating cycle, the subsequent cycle begins at $10^3/T = 13$ with a much lower conductivity. This annealing effect saturates at 150 K and the sample can be cycled reproducibly up and down the points shown (open triangles) until the film crystallizes near 200 K.

contains information about the temperature dependence of the energy gap and the density of states and mobility of charge carriers at the band edge.¹²

The temperature dependence of the conductivity of all of our annealed samples—regardless of composition—resembles that shown in Fig. 4. The values of ΔE and C for samples spanning the composition range studied are shown in Fig. 5. We find $0.14 \leq \Delta E \leq 0.17$ eV and $2 \times 10^2 \leq C \leq 10^3$ $\Omega^{-1} \text{cm}^{-1}$ with variation that appears to be experimental scatter rather than any compositional dependence of the high-temperature conduction mechanism. The error bars on the points shown for ΔE (solid circles) represent the uncertainty in fitting the $\sigma(T)$ data to a straight line. Error bars have been left off of the C data (open circles) for clarity, but these errors should be proportional to the corresponding errors on the ΔE points.

The behavior of the conductivity of our samples after annealing is what one might expect for the

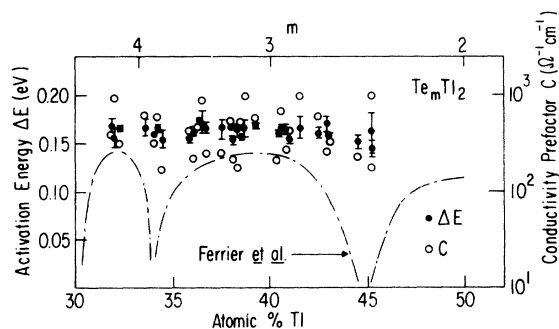


FIG. 5. Activation energy ΔE and conductivity prefactor C applicable for high-temperature conduction [$\sigma = C \exp(-\Delta E/kT)$] for films of Te_mTl_2 vs composition m . Both ΔE and C are composition independent for the films studied. The data of Ferrier *et al.* (Ref. 5) for activation energies is shown as the broken line. The error bars are left off of the data for C for clarity, but the uncertainty should be proportional to the corresponding error in measurement of ΔE for each composition.

Te-Tl system from the outset. That is, all bonds can be satisfied at all compositions and samples of different compositions might not be expected to have strongly different energy gaps. Thus charge transport in films of all compositions would be of similar character.

Because of the strong annealing effects, a measurement of the thermopower S of conductive films is not possible. Since any increase in temperature causes these films to anneal, the development of the gradient necessary to measure S causes annealing. Measurement of S for fully annealed samples is possible, however, and all of the films have positive S of roughly 1–2 mV/K. Again, the scatter in these values is not associated with composition.

B. Optical measurements

With the surprising results obtained in transport measurements in mind, we next investigate the optical properties of the Te-Tl system. For films prepared as described above we find no compositional dependence of the optical absorption or the index of refraction. In addition, the optical properties of all films are not affected by annealing prior to crystallization. Thus the anomalous behavior of the Te-Tl system is seen only in the low-temperature conduction of unannealed films. The optical data demonstrate the fact that the density of electronic states in the valence band and the conduction band are not noticeably affected as one proceeds from one composition to another. Hence the majority of the bands in the Te-Tl system are not a function of composition. The optical results

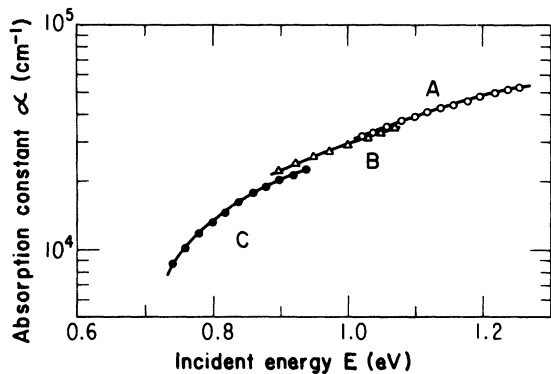


FIG. 6. Optical absorption constant α vs incident photon energy E for amorphous Te_mTl_2 of various compositions. $\alpha(E)$ for all compositions reproduce the curves shown for these three samples. From these data we find the energy at which $\alpha = 10^4 \text{ cm}^{-1}$ to be $E_{04} = 0.75 \pm 0.03 \text{ eV}$.

are shown in detail in Figs. 6–8 and are described below.

It is convenient to characterize the band gap of an amorphous semiconductor by determining the energy E_{04} at which the absorption constant $\alpha = 10^4 \text{ cm}^{-1}$. We show our data for α as a function of the energy of the incident radiation E for several samples in Fig. 6, and although only three samples are shown, these exhibit representative scatter in the data. For these coevaporated samples we find $E_{04} = 0.75 \pm 0.03 \text{ eV}$ —independent of composition. Samples of Te_mTl_2 where $1.8 \leq m \leq 3.8$ all have features identical to those shown in Fig. 6.

To assign a value to the optical energy gap, the absorption constant is expressed as a product of a matrix element times an integral over the joint density of states for the initial and final optical transition states. Assuming parabolic bands and performing the integration, one finds $\alpha E = (E - E_g)^2$ where E_g is the optical energy gap. In Fig. 7 we show plots of $(\alpha E)^{1/2}$ vs E for three samples of different compositions. Extrapolation of these data to $(\alpha E)^{1/2} = 0$ gives E_g . Again the samples shown display representative scatter of the data for films of all compositions. The values of E_g determined from such plots were $0.35 \leq E_g \leq 0.41 \text{ eV}$. Again there is no correlation between the optical band gap and composition.

The index of refraction n is likewise independent of composition over the entire spectral range studied (0.4–0.75 eV). In Fig. 8 we show the energy dependence of the index of refraction for films of many different compositions.

Upon annealing to the crystallization temperature T_c , the films become opaque within the sensitivity limit of our optical system (transmission $< 0.5\%$). For almost all films $T_c = 280 \pm 15 \text{ K}$. However, for

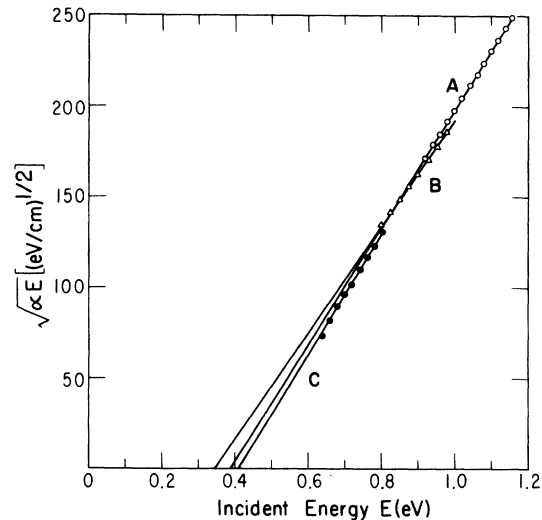


FIG. 7. $(\alpha E)^{1/2}$ vs incident photon energy E for amorphous Te_mTl_2 . Here α is the optical absorption constant. Extrapolation of these data to the intersection on the horizontal axis where $(\alpha E)^{1/2} = 0$ gives E_g , the optical energy gap.

films of Te_mTl_2 near half-integral m , T_c is measurably lower. That is, $T_c(m \sim 2.5, 3.5) = 170 \pm 20 \text{ K}$.

In one sense the transport and optical results described above give us a clearer picture of the nature of coevaporated samples of Te_mTl_2 , but in another sense they pose further problems. From the optical data we can conclude that the electronic band states are independent of composition. It appears as though the virgin samples near half-integral m compositions have considerably more defects or broken bonds than the samples near integral m . These defects give rise to a high density of localized gap states which can then be annealed

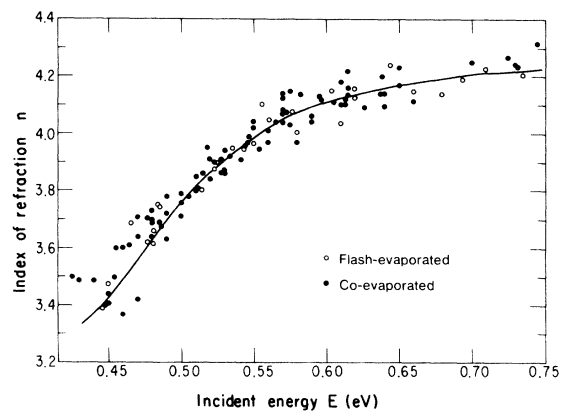


FIG. 8. Index of refraction n of amorphous Te_mTl_2 versus incident photon energy E for many different values of m . The index of refraction does not depend upon composition in this spectral range.

from the films. Since the gap is relatively small, only a small number of defect states are needed to raise the density of localized states at the Fermi level appreciably.

This filling in of the gap as one proceeds from m to $m + \frac{1}{2}$ would not be noticeable in the optical properties for the spectral range we investigated. At lower incident photon energies, these gap states would come into play, but in order to measure optical absorption in this region, thick samples (~ 1 mm thick) would be required. Such thicknesses could not be produced by vacuum deposition since the stresses built up during deposition would cause the film to peel from the substrate long before a thick enough layer could be grown.

The vanishing of the high conductivity for half-integral m samples upon annealing conflicts with the observation of FPA that annealing enhances differences in the conductivity. In order to resolve this conflict, we decided to reproduce the method of film preparation of FPA as closely as possible. They used a flash evaporation system in the manner described below.

C. Flash evaporated samples

From a description¹³ of the flash evaporation apparatus used in the studies of FPA, we built a system as shown in Fig. 9. Powders of grain size 125–177 μm were ground in the room atmosphere

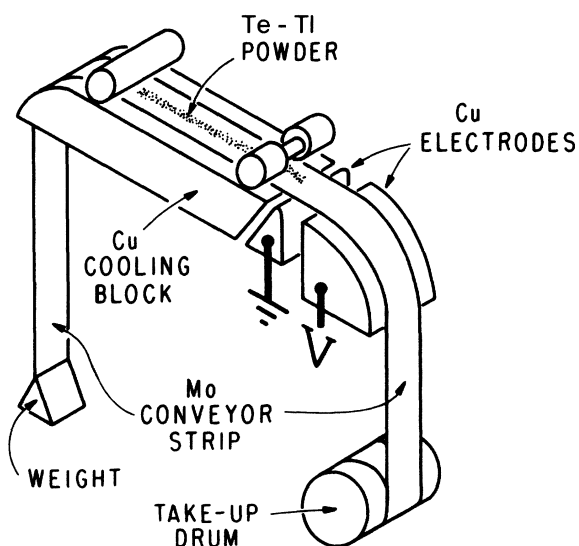


FIG. 9. Schematic drawing of the apparatus built to flash evaporate powders of Te-Tl. Mixed powder is placed on the molybdenum conveyor belt (0.002 in. thick) as shown. When current is passed from one electrode through the belt to the other electrode and the take-up drum is rotated, the powder is conveyed to the evaporation region where it flash evaporates.

at (50–70)% relative humidity from single pieces of Te and Tl. The powders were mixed in the desired ratio and placed on a 0.002-in.-thick molybdenum conveyor belt as shown in the figure. The system was evacuated within 15 min of grinding. Deposition conditions and charge material were identical to those used in coevaporation except that the deposition was monitored with one oscillator and kept at a rate of 50–100 $\text{\AA}/\text{sec}$. To deposit, a current of 60-A ac was passed through the portion of the conveyor belt touching the electrodes shown. When the take-up drum was rotated, the belt conveyed the powder into the evaporation region where it flash evaporated. As with the coevaporated samples, a composition calibration sample was included in each run. With this system the composition of the deposited film was the same as that of the mixed powder to within 2%.

The optical properties of the flash evaporated films are nearly identical to those of the coevaporated films. In particular, both of the measures of the optical energy gap (E_{04} and E_g) and the index of refraction (n) lie within the same ranges given above for coevaporated films. For flash evaporated films of compositions near half-integral m , however, the crystallization temperature T_c is higher than in the corresponding coevaporated film; specifically $T_c(m \sim 2.5, 3.5) = 240 \pm 15$ K. For integral m , T_c is the same for both types of films.

As before, similarities in optical properties reflect similarities in the principal bonding. That is, we conclude for flash evaporated samples as we did for coevaporated samples that the majority of the bonds in the system do not change as a function of composition. Furthermore, it is clear that flash evaporated and coevaporated samples are quite similarly bonded since their optical properties are essentially identical.

The conductivity σ of virgin flash evaporated samples of Te_mTl_2 is shown in Fig. 10. In this figure we have superposed the data for flash evaporated samples (shown as open circles) over the data for coevaporated films previously presented in Fig. 3. Once again the results of FPA for freshly deposited films are reproduced. Broad minima and sharp maxima occur at integral and half-integral m respectively. Upon annealing, however, we were surprised to find that the maxima persist in the annealed samples, i.e., the structure shown in the σ versus composition data of Fig. 10 exists for annealed as well as for virgin samples. Despite our conclusions in the previous paragraph that the principal bonding is the same for samples prepared by either technique, these conductivity data demonstrate that the structure of flash evaporated films is sufficiently dissimilar from coevaporated films to result in very different trans-

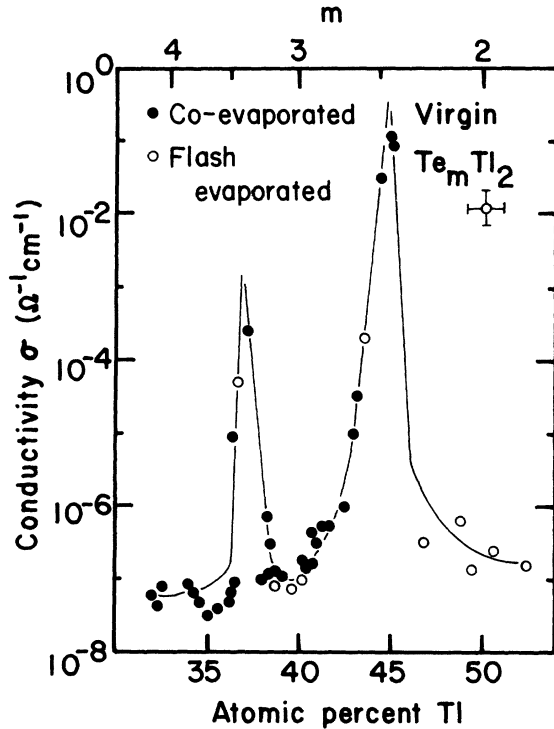


FIG. 10. Compositional dependence of the dc conductivity σ of flash evaporated samples of amorphous Te_mTl_2 . The flash evaporated samples are shown as open circles and are superposed on the data of Fig. 2 for coevaporated samples. For the flash evaporated samples, the features in these data persist for annealed samples. Typical error bars are shown in the open circle in the upper right.

port behavior.

The response of a relatively conductive sample to annealing is demonstrated in Fig. 11 where we plot $\log_{10} \sigma$ vs $(1/T)$. The virgin sample is relatively conductive and remains so through anneals to 105 and 167 K. Upon crystallization at 235 K, the sample becomes much more conductive. It was possible to cycle along similar curves for all of our flash evaporated samples of Te_mTl_2 at compositions near half-integral m . The resistive samples near integral m , on the other hand, behave very much like the resistive coevaporated samples. That is, $\sigma(T)$ resembles the fully annealed sample of Fig. 4.

One distinctive difference between our flash evaporated samples and those of FPA lies in the behavior of the conductivity of annealed films. This can best be seen by comparing Figs. 1 and 10. For the composition range covered in both figures ($2 \leq m \leq 4$), the behavior of the conductivity of virgin films from both laboratories is similar. However, upon annealing the conductivity of our flash evaporated films remains unchanged while that of

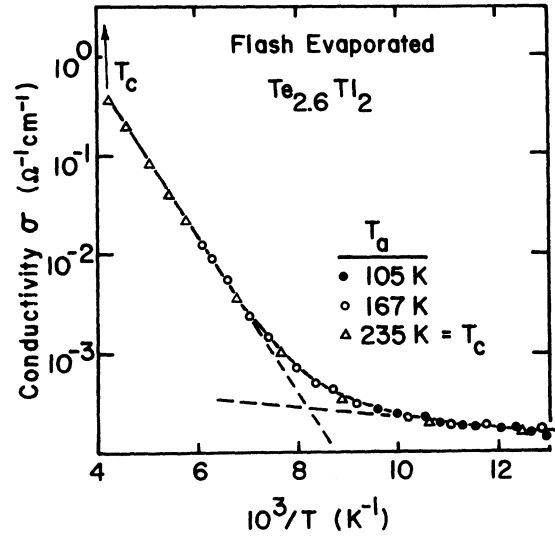


FIG. 11. Temperature T dependence of the dc conductivity σ of the flash evaporated amorphous $\text{Te}_{2.6}\text{Tl}_2$. No change in the behavior of σ is observed for samples annealed as shown. The film crystallizes at 235 K. Decomposition of σ into two terms as per Eq. (2) of the text is illustrated with the two dotted lines.

films of FPA change in the manner shown in Fig. 1. More precisely, FPA find for $2 < m < 2.5$ and $3 < m < 3.5$, that their films are unaffected by annealing while for $2.5 < m < 3$ and $3.5 < m < 4$, annealing results in a marked decrease of conductivity.

The resistive flash evaporated films (m integral) have positive thermopower for $95 \leq T \leq T_c$. The magnitude was generally between 0.4 and 1.0 mV/K over this range, and no single analytical form fit the $S(1/T)$ data for all samples. There was no correlation between the thermopower and composi-

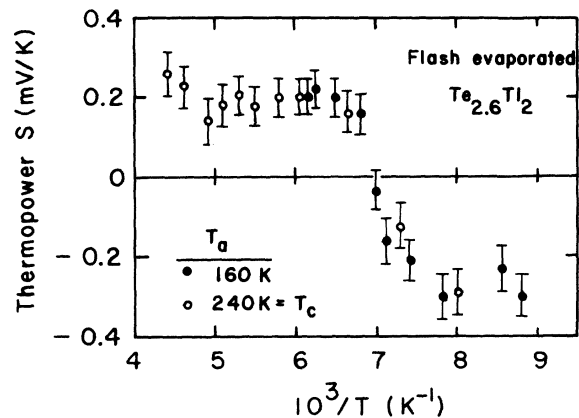


FIG. 12. Temperature dependence T of the thermopower S of flash evaporated amorphous $\text{Te}_{2.6}\text{Tl}_2$. S is positive for $10^3/T < 7$, but is negative for lower temperatures. The features shown here occur in all flash evaporated samples of Te_mTl_2 near half-integral m .

tion for these samples. At the conductivity maxima (m half-integral) all films exhibit thermopower behavior similar to that seen in Fig. 12. S is positive and rather small for $10^3/T < 7$. Then for lower temperatures, S changes sign and achieves a relatively temperature independent value of -0.2 mV/K.

In performing experiments aimed at explaining the properties of Te_mTl_2 associated with chemical ordering, we have here uncovered what might be an important clue to aid us. If we can explain why flash evaporated and coevaporated films behave differently in the manner described above, we may be led to a better understanding of chemical ordering and the role it plays in the amorphous Te-Tl system.

D. Oxidation studies

One difference between the two preparation methods used appears to be that in the FPA process of flash evaporation of powders from a conveyor belt, there is great likelihood of oxidation of the powders before the system is pumped down. The Tl powder in particular tarnishes noticeably from a shiny metallic to a dull grey appearance in the short time (15 min) needed to grind, weigh and transfer the powder. In coevaporation, on the other hand, the surfaces of molten Te and Tl appear to be clean and perhaps oxide-free. In addition the surface to volume ratio is much less for the charges used in coevaporation than for the grains of powder used in flash evaporation. The use of the Knudsen cell described above lends further support to the assertion that the coevaporated films are oxide-free.

To determine the amount of surface oxide on the flash evaporated powders, we must know the surface to volume ratio of the grains of powder and the mass added to clean surfaces of Te and Tl per unit surface area during the oxidation process. From the microscopic appearance of the powder grain size, shape and surface texture, we estimate the surface to volume ratio to be $5 \times 10^3 \text{ cm}^{-1}$.

To ascertain the rate of oxide growth on clean surfaces of Te and Tl we coevaporated films of each onto 5-MHz quartz crystal oscillators used as deposition monitors and measured the frequency shift upon exposing the oscillators to room air. The results of these experiments are shown in Fig. 13. The frequency decrease (and thus the mass increase per unit area) is plotted versus time t . At $t=0$ we admitted one atmosphere of dry nitrogen and observed a small shift of frequency most likely associated with the change in pressure. At $t=20$ min we admitted room air at 22°C and 55% relative humidity and observed a large fre-

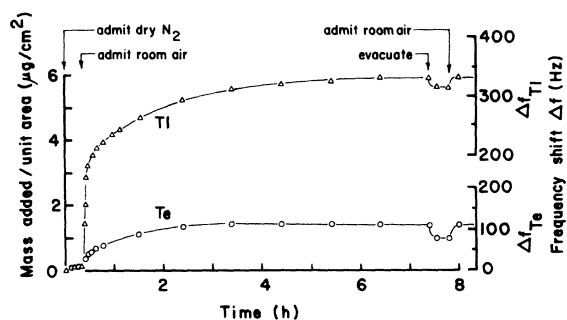


FIG. 13. Mass added per unit area of freshly deposited surfaces of Te and Tl versus time t after exposure to dry nitrogen and air. These data were obtained by measuring the frequency shift of 5 MHz quartz crystal oscillators onto which fresh films of Te and Tl had been deposited. At $t=0$ the surfaces were exposed to one atmosphere of dry nitrogen. At $t=20$ min, room air was admitted to the vacuum system and the subsequent oxidation saturated to 3 (6) h for the Te (Tl) surface. Between $t=7$ and $t=8$ h, the vacuum system was re-evacuated to determine the contribution of condensed water vapor to the observed frequency shift.

quency shift that saturates after 6 h for Tl and 3 h for Te. Oxidation after 15 min (the time it usually takes us to grind, weigh, and load the powder) is 70% of saturation for Tl and 50% for Te. To determine the amount of water adsorbed and unreacted on the surfaces, we reevacuated the system and measured the frequency shift due to its added mass. This shift can be seen on Fig. 13 between $t=7$ h and $t=8$ h. From the data of Fig. 13, we estimate the mass added per unit area of our powders to be $0.6 \mu\text{g}/\text{cm}^2$ for Te and $3.6 \mu\text{g}/\text{cm}^2$ for Tl.

From our estimates of the surface to volume ratio of the powder grains and the experimentally determined value of the mass added to clean Te and Tl surfaces upon oxidation, we estimate the oxygen content of the powders used in flash evaporation to be on the order of 1 at. %.

We checked these estimates of the oxygen content by performing Auger emission spectroscopy¹⁴ on both types of samples. Using a pressed powder sample of Te, Tl, and TeO_2 as a standard, we determined the oxygen content of the flash evaporated films to be 2–5 at. %. The coevaporated films are oxygen-free within the sensitivity limit of the Auger measurement (<0.5 at. %). By argon ion sputter etching in the Auger spectrometer, it was possible to obtain a depth profile of the films' compositions. Figure 14 shows a plot of the percent of each of the three constituents of 1- μm -thick films as a function of sputtering time. All films have a relatively uniform distribution of Te and Tl and as expected also a surface oxide that can be

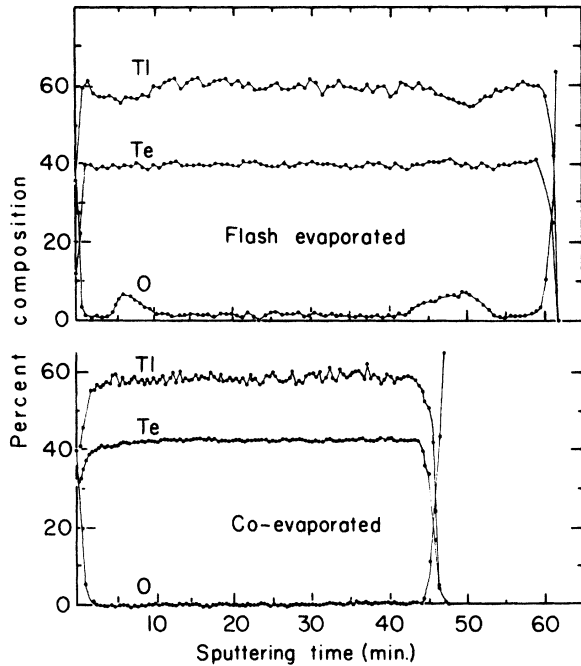


FIG. 14. Auger depth profile for flash evaporated and coevaporated films of amorphous Te_mTl_2 . The coevaporated film is oxygen-free while the flash evaporated film contains approximately 2–5-at.% oxygen. The oxygen content is not uniform through the depth of the flash evaporated film. Relatively weak Auger transition were monitored in order to allow the overall system gain to be operated at a high level. This improves the dynamic range of the instrument and maximizes the sensitivity for oxygen, but necessarily leads the noisy signals seen for Te and particularly Tl.

sputter etched from the film in 15–30 sec with an argon ion beam of 2×10^2 mA/cm². The oxygen content in the flash evaporated films is not uniformly distributed throughout the depth of the films. There are regions near the film-substrate interface as well as near the film-vacuum interface where the film is relatively oxygen-rich (~5-at.% oxygen). Throughout the bulk of the flash evaporated film, there is a uniform content of 1-at.% oxygen. It must be stressed that the Auger work was done after the films reached room temperature. Thus they were polycrystalline since the crystallization temperature is $T_c \sim 280$ K. We were not able to obtain Auger spectra on amorphous films since the films had to be removed from the deposition system and transported to the Auger spectrometer at room temperature. Thus it is impossible to tell whether the oxygen profile of the oxygenated films described above is a feature of the freshly deposited films, or whether it is due to subsequent migration of the oxygen upon annealing and crystallization.

IV. DISCUSSION

By correlating the information we have about the oxygen content of our films and their transport properties, we can begin to formulate a cohesive picture of the conduction process. It is plausible that as little as 2- or 3-at.% oxygen does not influence the measured optical properties since this amount of oxygen would not significantly alter the bonding of the material. On the other hand, such a small amount of oxygen could easily be sufficient to lock in localized gap states and prevent their annealing. This is particularly reasonable since these gap states are associated with defects and dangling bonds and this is precisely where one might expect oxygen to incorporate itself into the material.

Because crystalline order need not be conserved in a disordered system, the introduction of impurities into an amorphous semiconductor does not generally alter the properties of the material appreciably. This is so because the disordered matrix can adjust its bonds to accommodate the impurities and thereby satisfy all local bonding requirements.¹⁵ The introduction of impurities has been known, however, to affect crystallization. For example, a change in the crystallization process correlated with the presence of oxygen has been observed¹⁶ in thin films of amorphous germanium, but in this case crystallization at a given temperature is merely slowed down by the oxygen. Given this observation, it is not surprising that the crystallization temperature of Te_mTl_2 was found to be a function of oxygen content. However, it is remarkable that the presence of oxygen can so dramatically inhibit the annealing process.

It is most likely that our films and those studied by FPA contained significantly different amounts of oxygen. The differences observed in the annealing behavior discussed above (Sec. III C) is probably associated with different levels of oxygen impurities in the samples prepared in the two laboratories.

From the results presented in Fig. 11, it appears as though there are two distinct conduction regimes spanned by the data. We might express this by writing the conductivity as

$$\sigma = C \exp(-\Delta E/kT) + \sigma_1(T). \quad (2)$$

The two terms on the right in Eq. (2) are represented by the two dotted lines in Fig. 11. In the high-temperature regime, Eq. (2) reduces to Eq. (1) and the interpretation of the conduction process is quite straightforward. The value obtained for C is typical for conduction due to carriers excited into extended states. For this type of conduction in an amorphous semiconductor, it is quite often the

case that $\Delta E \sim \frac{1}{2}E_g$, and this is again true for our samples.

The low-temperature conduction is not so easily interpreted for several reasons. Not the least of these is the fact that our data spans so narrow a range of conductivities that the exact temperature dependence of σ_1 is impossible to ascertain.

The first of our *a priori* explanations of the behavior of the low-temperature charge transport in Te_mTl_2 has clearly been ruled out, i.e., σ_1 cannot be described in terms of differences in bonding between integral and half-integral m materials. It also seems clear that the origin of the conductive behavior given by σ_1 is probably not a manifestation of a charge transfer system as proposed at the outset of our investigation. This is so because the thermopower is composition independent for most of our oxygenated samples. We cannot rule out charge transfer completely, however, since the thermopower often exhibits exceptional behavior in small band-gap materials.¹⁷ For example in amorphous $\text{Tl}_2\text{Te} \cdot \text{As}_2\text{Te}_3$, Nagels *et al.*¹⁸ find $\Delta E = 0.25$ eV while the activation energy determined from the slope of S against $1/T$ is 0.13 eV.

Because of the relative temperature independent behavior of σ_1 , we can conclude that conduction in the low-temperature regime takes place near the Fermi level E_F . This situation may have arisen because of a movement of E_F towards one of the bands. But this would require donors in the upper half of the gap (since the thermopower is negative) and the absence of any other gap states of sufficient number to pin E_F near mid-gap. A more physical explanation is that the conduction process has moved to the Fermi level, i.e., to mid-gap.

Two distinct transport processes are known to occur when conduction takes place at E_F in amorphous semiconductors. The first of these is nearest-neighbor hopping^{19,20} and results in a conductivity given by

$$\sigma_1(T) \propto \exp(-\epsilon_3/kT), \quad (3)$$

where ϵ_3 is the average energy difference between nearest neighbors. The other process is variable range hopping²¹ and its temperature dependence can be expressed as

$$\sigma_1(T) \propto \exp[-(T_0/T)^{1/4}]. \quad (4)$$

Here T_0 is a function of the density of states at the Fermi level and the spatial extent of the localized wave functions of the electronic gap states. As stated above, it is not possible to determine the exact temperature dependence of σ_1 so we cannot distinguish between these two processes in our data. We can, however, fit the low-temperature conductivity data for oxygen-doped samples at con-

ductivity maxima to expression (3) and (4) to determine if the resulting values of ϵ_3 and T_0 are reasonable.

For nearest-neighbor hopping, we find ϵ_3 to be of the order of 1 meV. This value lies in the range of the theoretically and experimentally determined values^{19,20} for nearest-neighbor hopping energies.

Fitting the data of Fig. 11 to Eq. (4) for variable range hopping, we find $T_0 \sim 2 \times 10^6$ K. This value is relatively small, but is certainly a physically reasonable value similar to that found in other amorphous semiconductors.²²⁻²⁴

In referring again to Fig. 5, we can now understand the apparent discrepancy between our results and those of FPA who show a compositional dependence of the activation energy as shown with the broken line. FPA have here referred to the low-temperature conduction as an activated process, thus obtaining activation energies as low as 1 meV. The true high-temperature activation energies of FPA closely resemble our data as shown in Fig. 5.

Although we cannot determine the exact nature of the conduction given by $\sigma_1(T)$, the abruptness of the transition from band conduction to localized state conduction can shed light on the density of electronic gap states. In other amorphous semiconductors in which a change to nonintrinsic conduction has been observed at low temperatures,²⁵ the change of slope on the σ -vs- $1/T$ plot is more gradual than that seen in Fig. 11. For such semiconductors one generally pictures the conduction mechanism as sliding gradually into the pseudogap as the temperature is lowered. In the high-temperature regime, intrinsic conduction takes place in the bands and the activation energy is constant over a large temperature range. As the amorphous semiconductor is cooled, a temperature is reached at which sufficient thermal energy is not available to excite charge carriers from the Fermi level to the extended states at the mobility edge and the activation energy begins to decrease. At this temperature, conduction takes place in the pseudogap very near the mobility edges. As still lower temperatures are reached, the states contributing to the conduction lie further and further into the pseudogap and the activation energy decreases more. As the conduction mechanism approaches the Fermi level at still lower temperatures, the conduction becomes very weakly temperature dependent. At these temperatures, a hopping model is frequently employed to account for the temperature dependence of the conductivity. Redfield²⁶ has analytically examined the temperature dependence of the conduction in terms of a model in which the conduction process behaves in the manner described. For a model with no features in the den-

sity of electronic gap states, he finds a gradual change in the slope of the σ -vs- $1/T$ plot.

The conductivity of Te_mTl_2 for half-integral m behaves much differently. In Fig. 11 an abrupt change is seen to occur in the slope of the σ -vs- $1/T$ plot. It appears, therefore, that as the temperature is lowered the conduction mechanism jumps suddenly in energy from extended states near the mobility edge to localized states at the Fermi level. These data imply that a peak exists in the density of electronic gap states at the Fermi level. Such a model has been proposed by Davis and Mott.²⁷ We find such a picture of the electronic density of states to be quite reasonable for amorphous films of Te_mTl_2 at half-integral m .

From the results of our experiments we now have a more complete picture of amorphous Te_mTl_2 and should reassess our initial view of the system as being strongly chemically ordered. Certainly the compositional dependence of the conductivity σ shown in Fig. 10 is among the most dramatic compositional effects ever observed in an amorphous system. The regularity of the behavior of σ when plotted versus m initially leads one to assume that the solid is composed of molecular aggregates of Te_mTl_2 with integral m . The activation energies as published by FPA (Fig. 5) lend further weight to the assertion that fundamental changes occur in Te_mTl_2 as the composition is varied from one integral value of m to the next. We have now shown, however, that this interpretation of the temperature dependence of the conductivity is mistaken.

The extreme fluctuations seen in Fig. 10 occur in the low-temperature regime where conduction is dominated by a relatively small number of localized electronic gap states. A few atomic percent of oxygen can strongly alter the annealing behavior of these few states. The fluctuations of σ are actually subtle changes in the overall density of electronic states but since we examine the conductivity in a low-temperature regime, these changes appear in an exponential manner. Our optical data further emphasizes the fact that the principal features of bonding and transport in amorphous Te_mTl_2 are not composition dependent.

Generally when one speaks of chemical ordering in an amorphous system, one observes changes in the high-temperature activation energy²⁸ as a function of composition. As seen in Fig. 5, the activation energies of Te_mTl_2 are not a function of composition. It is the low-temperature tail of Fig. 11 that has strong compositional dependence. Thus when we speak of chemical ordering in the amorphous Te-Tl system we must point out that despite the remarkable behavior of the compositional dependence of the low-temperature conduction, the

system is not strongly chemically ordered in the usual sense of the term.

Although we now have a more complete picture of conduction in thin films of amorphous Te_mTl_2 , we have not solved the problem of why the density of defects or dangling bonds is higher for half-integral m compositions. We have, however, uncovered an equally exciting problem. Namely, how does the presence of oxygen affect the localized gap states. We have found that a few atomic percent of oxygen drastically affects the annealing behavior of defect states. The interaction of oxygen with these states gives us one of our first real handles on the chemistry of localized states in amorphous semiconductors. A more complete study of the effects of oxygen on the transport properties of this system may reveal much about the nature of localized gap states in amorphous semiconductors.

A more exact determination of the temperature dependence of the low-temperature conduction for films of half-integral m would also help in this regard. Determination of the temperature dependence of σ_1 down to liquid-helium temperatures should certainly prove to be an informative investigation.

V. CONCLUSION

The published data on the dc conductivity of thin amorphous films of $\text{Te}_x\text{Tl}_{1-x}$ present one with problems basic to the understanding of chemical bonding and charge transport in amorphous semiconductors. Starting with models proposed to account for the behavior of these films, we designed several experiments aimed at establishing the validity of each model. Although the results of our investigations established that neither of our models accurately portrays the physical origin of the observed properties of the system, we were led to interesting new insights into the structure of the electronic density of states of the system. This in turn led us to other experiments aimed at further elucidating this density of states and ultimately we emerged with a clearer picture of charge transport in amorphous $\text{Te}_x\text{Tl}_{1-x}$ films.

We found that the bonding in the Te-Tl system is not a function of composition and that doping with several atomic percent of oxygen does not significantly alter this bonding. The strong compositional dependence of the conductivity is due to a peak in the density of electronic gap states that occurs at compositions corresponding to half-integral m in films of Te_mTl_2 . These gap states can be removed from pure films upon annealing, but the introduction of a few atomic percent oxy-

gen can succeed in locking the states into the system even for annealed samples. Our results have shown that despite the dramatic fluctuations seen in the compositional dependence of the low-temperature dc conduction, the amorphous Te-Tl system is not strongly chemically ordered in the usual sense of the term.

Further investigation of this unique system could quite possibly lead to new insights into the nature of localized states in amorphous semiconductors. For example, a controlled oxygen-doping study might yield fruitful information about the chemistry of defect states or dangling bonds. Coupled with such a study, efforts to measure the conductivity at lower temperature should be undertaken to better characterize the low-temperature charge transport mechanism.

ACKNOWLEDGMENTS

The author would like to express his gratitude to Professor H. Fritzsche for his encouragement and continued guidance throughout the work. The initial stages of this study (transport measurements on coevaporated samples) were undertaken in collaboration with Dr. Al \acute{e} s Triska, who at the time was a visiting scientist sponsored by the Czechoslovakian Academy of Sciences. The author gratefully acknowledges the many contributions of Dr. Triska. Thanks are due to David Dennison for his help in solving some of the experimental difficulties encountered, to Dr. Jun Ito for his assistance in determining the composition of our samples, and to the personnel of the University of Illinois Materials Research Laboratory where the Auger spectroscopy was performed.

† Work supported by NSF DMR75-15003. We have also benefited from support of the Materials Research Laboratory by the NSF.

* Submitted in partial fulfillment of the requirements for a Ph.D. degree in the Dept. of Physics, The University of Chicago.

‡ Present address: Max-Planck-Institut für Festkörperforschung, 7 Stuttgart 80 Federal Republic of Germany.

¹R. P. Ferrier, J. M. Prado, and M. R. Anseau, *J. Non-Cryst. Solids* **8-10**, 798 (1972).

²L. Pauling, *The Nature of the Chemical Bond* (Cornell U. P., Ithica, N. Y., 1960).

³J. Cornet and D. Rossier, *Philos. Mag.* **27**, 1335 (1973).

⁴John P. de Neufville, *J. Non-Cryst. Solids* **8-10**, 85 (1972).

⁵See, for example, S. Tsuchihashi and Y. Kuwamoto, *J. Non-Cryst. Solids* **5**, 286 (1971); K. Arai, T. Kuwahata, H. Namikawa, and S. Saito, *Jpn. J. Appl. Phys.* **11**, 1080 (1973); M. B. Myers and E. J. Felty, *Mater. Res. Bull.* **2**, 535 (1967).

⁶M. Cutler, *Philos. Mag.* **24**, 381 (1971).

⁷M. Cutler, *Philos. Mag.* **24**, 401 (1971).

⁸J. P. de Neufville, *Optical Properties of Solids—Recent Developments*, edited by E. O. Seraphin (North-Holland, Amsterdam, 1975).

⁹M. Knudsen, *Ann. Phys.* **29**, 179 (1909).

¹⁰Palladium electrodes were chosen for ease of fabrication and the absence of any evidence of palladium alloying with Te. For a discussion of choice of electrode material, see H. Y. Wey, *Phys. Rev. B* (to be published).

¹¹A preliminary report appears as H. Fritzsche, M. A. Paesler, and A. Triska, *Bull. Am. Phys. Soc.* **20**, 322 (1975).

¹²The general references for this paper are: *Amorphous and Liquid Semiconductors*, edited by J. Tauc (Plenum, New York, 1974); *Electronic Processes in Non-Crystalline Materials*, edited by N. F. Mott and E. A. Davis

(Clarendon, Oxford, 1971); *Electronic and Structural Properties of Amorphous Semiconductors*, edited by P. G. LeComber and J. Mort (Academic, New York, 1973).

¹³J. M. Prado, Ph.D. thesis (University of Cambridge, 1972) (unpublished).

¹⁴The Physical Electronics Model No. 545 Scanning Auger Microprobe of the University of Illinois Materials Research Laboratory was used.

¹⁵Exciting new work in the doping of amorphous semiconductors has recently been carried out by W. E. Spear and P. G. LeComber, *Solid State Commun.* (to be published).

¹⁶A. Barna, P. B. Barna, and J. F. Pocza, *J. Non-Cryst. Solids* **8-10**, 36 (1972).

¹⁷H. Fritzsche, in *Amorphous and Liquid Semiconductors*, edited by J. Tauc (Plenum, New York, 1974), p. 221.

¹⁸P. Nagels, R. Collaerts, M. Denayer, and R. DeConinck, *J. Non-Cryst. Solids* **4**, 295 (1970).

¹⁹H. Fritzsche, *Phys. Rev.* **99**, 406 (1955).

²⁰H. Fritzsche, *J. Phys. Chem. Solids* **6**, 69 (1958).

²¹N. F. Mott, *Philos. Mag.* **19**, 835 (1969).

²²H. Dover, O. Massenet and B. K. Chakraverty, *Solid State Commun.* **11**, 131 (1972).

²³J. J. Hauser, *Phys. Rev. B* **8**, 2678 (1973).

²⁴J. J. Hauser, *Phys. Rev. B* **9**, 2623 (1974).

²⁵For example, H. Mell discusses the behavior of tetrahedrally bonded amorphous semiconductors in *Amorphous and Liquid Semiconductors*, edited by J. Stuke and W. Brenig (Wiley, New York, 1974).

²⁶David Redfield, *Phys. Rev. Lett.* **27**, 730 (1971).

²⁷E. A. Davis and N. F. Mott, *Philos. Mag.* **22**, 903 (1970).

²⁸See for example, H. F. Uphoff, and J. H. Healy, *J. Appl. Phys.* **32**, 950 (1961); L. Štourač, A. Abraham, A. Hruby, and M. Zavetova, *J. Non-Cryst. Solids* **8-10**, 353 (1972).